

# New age constraints on Aptian evaporites and carbonates from the South Atlantic: Implications for Oceanic Anoxic Event 1a

Leonardo R. Tedeschi<sup>1,2\*</sup>, Hugh C. Jenkyns<sup>1</sup>, Stuart A. Robinson<sup>1</sup>, Antonio E.S. Sanjinés<sup>2</sup>, Marta Claudia Viviers<sup>2</sup>, Cláudia M.S.P. Quintaes<sup>3</sup>, and Joselito C. Vazquez<sup>2</sup>

<sup>1</sup>Department of Earth Sciences, University of Oxford, South Parks Road, Oxford OX1 3AN, UK

<sup>2</sup>Petrobras, Research Center (CENPES, Centro de Pesquisas Leopoldo Américo Miguez de Mello), Avenida Horácio Macedo, 950, Ilha do Fundão, Cidade Universitária, Rio de Janeiro-RJ, 21941-915, Brazil

<sup>3</sup>Petrobras, Exploration and Production (E&P), Avenida República do Chile, 330, Rio de Janeiro-RJ, 20031-170, Brazil

## ABSTRACT

**High-resolution carbon isotope ( $\delta^{13}\text{C}$ ) profiles from shallow- and deep-water carbonates in the South Atlantic (Campos and Santos Basins) are here correlated to stratigraphically well calibrated Tethyan sections, constraining the end of major evaporite deposition in the South Atlantic to the early Aptian Oceanic Anoxic Event (OAE) 1a interval. The unusually extensive evaporite deposition would have reduced the global dissolved sulfate inventory, possibly increasing global preservation of organic matter by decreasing sulfate reduction; this could explain the coincidence in timing between OAE 1a and the dramatic negative sulfur isotope excursion over this interval. Therefore, in addition to the coeval eruption of the Ontong Java Plateau, the opening of the South Atlantic may have played an important role in the genesis and character of OAE 1a.**

## INTRODUCTION

Oceanic anoxic events (OAEs) are time intervals when oxygen depletion characterized much of the middle and/or deeper waters of the world's oceans. As a result, an unusual amount of organic matter was preserved in marine sediments worldwide (Jenkyns, 2010). OAE 1a is typically identified by an organic-rich sedimentary record and/or characteristic carbon isotope signature ( $\delta^{13}\text{C}$ ) in carbonate or organic matter: phenomena recorded in geographically widespread localities (Menegatti et al., 1998; Bottini et al., 2015). Possible causative mechanisms include accelerated input of nutrients from basalt-seawater interaction, massive  $\text{CO}_2$  release from extrusion of the Ontong Java Plateau, and/or dissociation of methane hydrate (Méhay et al., 2009; Bottini et al., 2012, 2015).

The evaporites from the central segment of the South Atlantic Ocean (Fig. 1) are conventionally considered to be in the age range 116–111 Ma, based on Ar–Ar ages from the subevaporite volcanic sequence (e.g., Davison, 2007; Chaboureaux et al., 2013), and to be unrelated to OAE 1a, dated as ca. 125–120 Ma (e.g., Bottini et al., 2015; Ogg et al., 2012). However, the existing dates for the evaporites are problematic. The aim of this study is to constrain the age of these deposits in southern Brazilian basins by using new foraminiferal biostratigraphy and  $\delta^{13}\text{C}$  data from supraevaporite carbonates from

Petrobras-cored well CB-3 in the Campos Basin and published  $\delta^{13}\text{C}$  data from Petrobras wells CP-5 (Campos Basin) and X (Santos Basin), from below and above the evaporites, respectively (Dias, 1998; Quintaes, 2006) (Figs. 1 and 2).

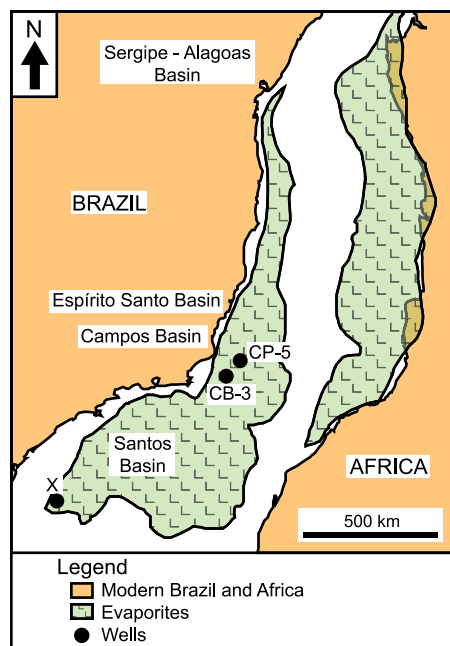


**Figure 1. Location map of offshore Petrobras wells CB-3 and CP-5 and X, southeast Brazil. Reconstruction between Brazil and Africa to 113 Ma after evaporite deposition is adapted from Norton et al. (2016).**

## METHODS

Petrobras well CB-3 is located in the offshore Campos Basin (22°44'S, 40°40'E) (Fig. 1) and terminated an unknown distance above the evaporites (Fig. 2). We prepared and analyzed 171 core samples (from depth interval 2484–2689 m) for foraminiferal biostratigraphy in the Research Center of Petrobras (Rio de Janeiro, Brazil), using concepts from Premoli Silva and Verga (2004) and Huber and Leckie (2011). We analyzed 195 core samples (from depth interval 2437–2689 m) for carbon and oxygen isotopes ( $\delta^{13}\text{C}$  and  $\delta^{18}\text{O}$ ) on bulk carbonate. Data are reported in parts per thousand (‰) relative to the Vienna Pee Dee belemnite standard. The International Atomic Energy Agency CO-1 standard gave a standard deviation ( $\sigma$ ) of  $\pm 0.07\text{‰}$  for  $\delta^{13}\text{C}$  and  $\pm 0.12\text{‰}$  for  $\delta^{18}\text{O}$ . We also compiled  $\delta^{13}\text{C}$  and total organic carbon (TOC) values from cuttings from supraevaporite Petrobras well X, Santos Basin (Quintaes, 2006), and subevaporite Petrobras well CP-5, Campos Basin (Dias, 1998), to generate composite carbonate carbon isotope and TOC curves (Santos–Campos composite), where original samples were not available for further analyses. All results, detailed methods, quality control, and compilation of data are provided in the GSA Data Repository<sup>1</sup>.

## GEOLOGICAL SETTING OF THE SANTOS AND CAMPOS BASINS

The Santos and Campos Basins formed during the opening of the central segment of the South Atlantic Ocean in the Early Cretaceous (Davison, 2007; Chaboureaux et al., 2013). The stratigraphic record, based on offshore wells, is divided into three main supersequences, rift, postrift, and drift, as described by Moreira et al. (2007) and Winter et al. (2007). Above the basement, the rift supersequence comprises volcanic rocks, continental siliciclastics, and

<sup>1</sup>GSA Data Repository item 2017169, detailed methods, Figures DR1–DR3 and Tables DR1 and DR2 with all geochemical data obtained in this study, is available online at <http://www.geosociety.org/datarepository/2017/> or on request from [editing@geosociety.org](mailto:editing@geosociety.org).

\*E-mail: [leonardo@earth.ox.ac.uk](mailto:leonardo@earth.ox.ac.uk), [leonardo.tedeschi@petrobras.com.br](mailto:leonardo.tedeschi@petrobras.com.br)

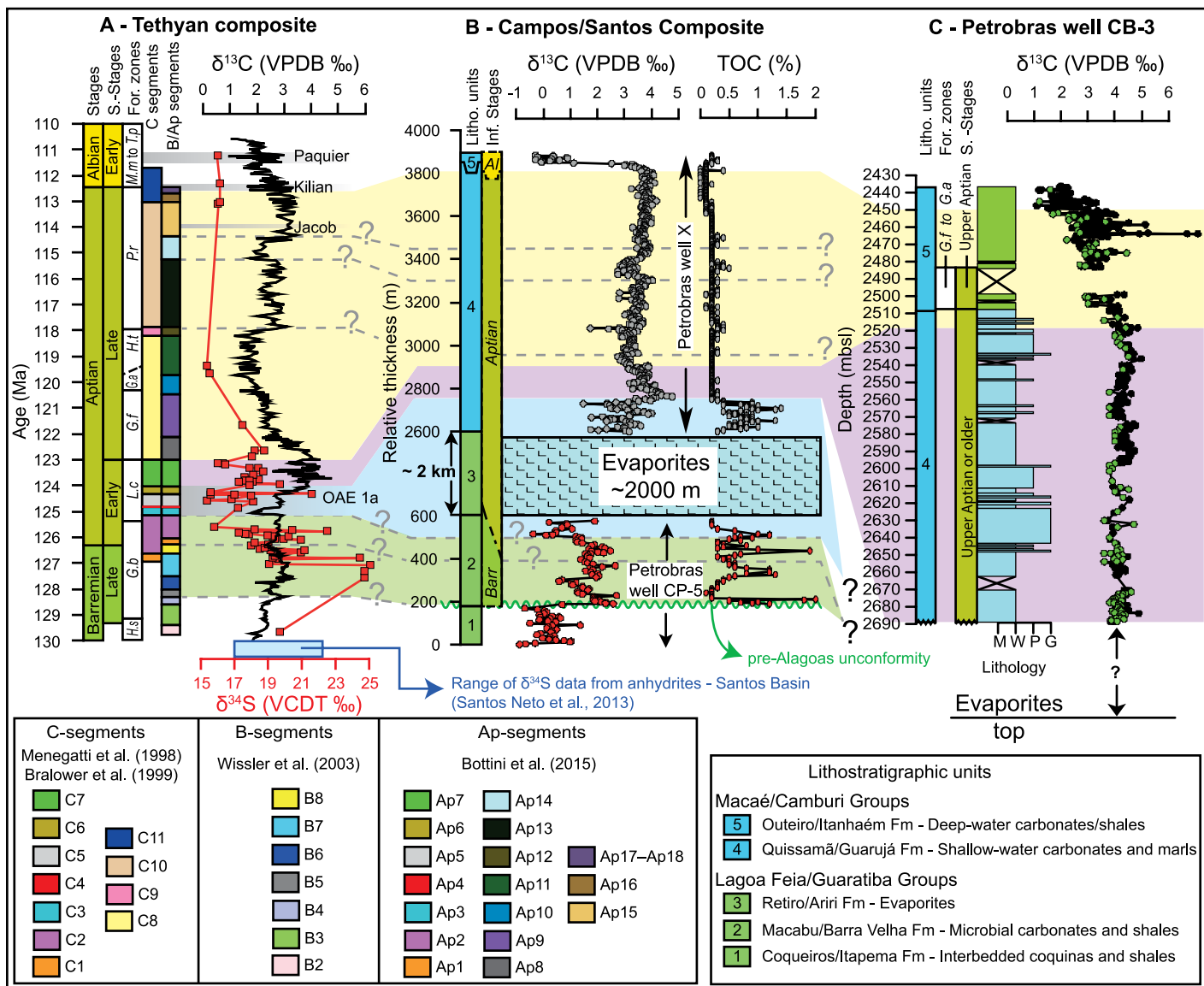


**Figure 2. Chemostratigraphic correlations.** A: Tethyan carbonate carbon isotope composite age-calibrated curve (Ogg et al., 2012). Black indicates carbonate carbon isotope composite from Herrle et al. (2015); red squares are  $\delta^{34}\text{S}$  from Ocean Drilling Program Site 766A, Permanent section and Cismon core (Paytan et al., 2004; numerical age adjusted to time scale of Ogg et al., 2012, after Gomes et al., 2016); gray shows organic-rich levels Jacob, Killian, Paquier, and Oceanic Anoxic Event 1a (OAE 1a). VPDB—Vienna Peedee belemnite; VCDT—Vienna Canyon Diablo troilite. B: Campos-Santos carbonate carbon isotope and total organic carbon (TOC) composite curve displayed in relative thicknesses based on Petrobras wells CP-5 (red circles) and X (gray circles). Note the break in the y-axis to include as much as 2 km of evaporites, as estimated by Davison et al. (2012). TOC values higher than 2% are omitted in this diagram (four samples from Petrobras well CP-5). C: Petrobras well CB-3: lithostratigraphic units, foraminiferal zones, substages, lithology (M—mudstone, W—wackestone, P—packstone, G—grainstone), and carbon isotope data (black—this study; green—Azevedo, 2001). Green, blue, purple, and yellow bands and gray dashed lines show suggested correlation between A, B, and C, where the base of the evaporites could be older than OAE 1 (see text for details). Abbreviations: Inf—inferred, Barr—Barremian, U. Ap—upper Aptian, Al—Albian, S-stages—substages, mbsl—meters below sea level, Litho.—lithology, For.—foraminiferal, Fm—formation. Foraminifera: *H.s.*—*Hedgerbella similis*, *G.b.*—*Globigerinelloides blowi*, *L.c.*—*Leupoldina cabri*, *G.f.*—*Globigerinelloides ferreolensis*, *G.a.*—*Globigerinelloides algerianus*, *H.t.*—*Hedgerbella trocoidea*, *P.r.*—*Paraticinella rohri*, *M.m.*—*Microhedgerbella miniglobularis*, *T.p.*—*Ticinella primula*.

interbedded lacustrine coquinas and organic-rich shales (Coqueiros and Itapema Formations; Fig. 2); in distal settings, the overlying postrift supersequence comprises interbedded microbial carbonates and shales (Macabu and Barra Velha Formations; Fig. 2). The evaporites terminate the postrift supersequence and comprise cycles of predominantly anhydrite and halite, locally with more soluble salts such as carnallite, sylvite, and tachyhydrite (Retiro and Ariri Formations;

Fig. 2). Halite and anhydrite from the Espírito Santo Basin, north of the Campos Basin (Fig. 1), have Br contents and  $^{87}\text{Sr}/^{86}\text{Sr}$  ratios that indicate derivation from marine waters (Dias, 1998). The anhydrite probably formed from dewatering of gypsum during burial and shows textures typical of precipitation in subaqueous settings, such as thin laminations and twinned crystals, as well as nodules of probable sabkha facies (Dias, 1998). Above the evaporites, in distal settings,

the early drift supersequence is represented by shallow-marine platform carbonates (Quissamã and Guarujá Formations; Fig. 2) containing planktonic foraminiferal species that are not age diagnostic (e.g., *Favusella ex grege washitensis*; Azevedo et al., 1987). Following platform drowning, deeper water sediments accumulated (Outeiro and Itanhaém Formations; Fig. 2), in which Aptian and younger calcareous nannofossils (e.g., *Nannoconus truitii*) and planktonic

foraminifera are present (e.g., *Globigerinelloides ferreolensis*; *Ticinella raynaudi*; Azevedo et al., 1987; this study).

## RESULTS AND STRATIGRAPHIC CORRELATION WITH REFERENCE SECTIONS

An assemblage of 11 planktonic foraminifera (*Hedbergella aptiana*, *H. gorbachikae*, *H. infractacea*, *H. sigali*, *H. luterbacheri*, *H. tuschepsensis*, *H. kuznetsovae*, *H. occulta*, *G. ferreolensis*, *G. barri*, and *Favusella ex grege washitensis*) was identified from 2484 to 2508 m from Petrobras well CB-3. This assemblage indicates the upper Aptian from the *G. ferreolensis* to the *G. algerianus* zones (cf. Premoli Silva and Verga, 2004; Ogg et al., 2012) (Fig. 2; Fig. DR1 in the Data Repository). Samples below 2508 m, deposited in relatively shallow water, contain a low-diversity assemblage with relatively long ranging species of benthic (e.g., *Lenticulina ex grege nodosa*) and planktonic foraminifera (ex. *Favusella ex grege washitensis*), and are interpreted as early-late Aptian or older.

The carbon isotope profile from Petrobras well CB-3 shows a defined pattern (Fig. 2): a stratigraphically lower section (2689–2517 m) showing relatively high  $\delta^{13}\text{C}$  values (3.60‰–4.97‰) and a stratigraphically higher section (2517–2437 m) that shows a trend of decreasing  $\delta^{13}\text{C}$  values from bottom (3.0‰–3.3‰) to top (1.2‰–1.6‰), interrupted by a positive excursion with values >4‰. Relatively high  $\delta^{13}\text{C}$  values, as in the interval 2689–2517 m, characterize part of the so-called C7/Ap7 isotopic segment (latest early Aptian–earliest late Aptian interval), with the highest  $\delta^{13}\text{C}$  values of the Aptian stage (e.g., Menegatti et al., 1998; Bottini et al., 2015) (purple band in Fig. 2). Although no biostratigraphic constraints are available stratigraphically above 2484 m, the trend of decreasing  $\delta^{13}\text{C}$  values and positive excursion, as in the interval 2517–2450 m, are similar to the C8–C10/Ap8–Ap15 segments of the late Aptian (cf. Bralower et al., 1999; Bottini et al., 2015) (yellow band in Fig. 2). Deeper water sediments stratigraphically above 2450 m do not have biostratigraphic constraints and do not show diagnostic  $\delta^{13}\text{C}$  patterns. They are here interpreted as latest late Aptian or younger in age.

The Santos-Campos composite (Fig. 2) does not have any biostratigraphic constraints based on planktonic marine fossils, and this correlation with the Tethyan reference section is based on  $\delta^{13}\text{C}$  values. The basal interval (0–173 m) lacks diagnostic features on the  $\delta^{13}\text{C}$  curve and it is stratigraphically below an important regional unconformity identified in seismic lines and other oil wells in southern Brazilian basins called the pre-Alagoas unconformity (Dias, 1998; Fig. 2). Therefore, it cannot be correlated with the Tethyan reference curve. The stratigraphically higher subevaporite interval 186–501 m,

with  $\delta^{13}\text{C}$  generally in excess of 1.2‰, is tentatively correlated with upper Barremian B5–B8 segments and lower Aptian Ap1–Ap2 segments (green band in Fig. 2; Wissler et al., 2003; Bottini et al., 2015); the subevaporite interval 501–573 m, with  $\delta^{13}\text{C}$  generally <1.2‰, is tentatively correlated with the C3/Ap3 segment that characterizes the base of the OAE 1a interval worldwide (cf. Menegatti et al., 1998; Bottini et al., 2015) (blue band in Fig. 2). However, the correlations of the interval 186–573 m are tentative, especially the lower values found in the interval 501–573 m, because of deposition in continental environments (e.g., Sabato Ceraldi and Green, 2017) and/or diagenetic overprints.

Above the evaporites, the interval 2600–2756 m shows a general trend of increasing  $\delta^{13}\text{C}$  values typical of the C6/Ap6 segments and TOC values as high as 1.4‰ (cf. Menegatti et al., 1998; Bottini et al., 2015) (blue band in Fig. 2), geochemical characteristics that likely constrain this interval to the latter part of OAE 1a. The highest  $\delta^{13}\text{C}$  values (3.14‰–4.77‰) from the Santos-Campos composite (2756–2906 m) are diagnostic of the Aptian immediately post-OAE 1a sediments of the C7/Ap7 segment (cf. Menegatti et al., 1998; Bottini et al., 2015) (purple band in Fig. 2). The interval 2906–2948 m (basal part of yellow band in Fig. 2) shows a trend of decreasing  $\delta^{13}\text{C}$  values that may record the lower part of the C8–Ap8 segment (cf. Bralower et al., 1999; Bottini et al., 2015). The Campos-Santos composite does not show the lower  $\delta^{13}\text{C}$  values and subsequent increasing trend of  $\delta^{13}\text{C}$  values (C8–C9/Ap8–Ap16 segments; Bralower et al., 1999; Bottini et al., 2015) present in the Tethyan reference curve (Fig. 2; time scale of Ogg et al., 2012). It is significant that the Ap8–Ap11 segments are apparently extremely condensed or possibly missing. The broad positive excursion in the interval 2948–3803 m has been observed in upper Aptian sediments worldwide (C10/Ap13–Ap15 segments; Bralower et al., 1999; Bottini et al., 2015) (yellow band in Fig. 2). Because we lack biostratigraphic analyses of the shallow- and deep-water carbonates above 3803 m, they are interpreted as latest late Aptian or younger in age.

## STRATIGRAPHY OF SOUTH ATLANTIC EVAPORITES

The evidence suggests that the top of the evaporites correlates with the upper part of the OAE 1a interval and that most of the postevaporite shallow-water carbonates are Aptian in age; this constitutes a major stratigraphic revision of southern Brazilian basins. Deposition of the South Atlantic evaporites is estimated to have lasted 400–600 k.y., based on cyclostratigraphy, and the reconstructed depositional rate of ~5 mm yr<sup>-1</sup> is similar to modern evaporite depositional rates from Lake Assal, Africa (10 mm yr<sup>-1</sup>), MacLeod Basin evaporites, western Australia

(4–100 mm yr<sup>-1</sup>), and Messinian evaporites of the Mediterranean (6.6 mm yr<sup>-1</sup>) (Dias, 1998; Davison et al., 2012, and references therein). Therefore, it is likely that the formation of South Atlantic evaporite body was shorter than the duration of OAE 1a (~1.1 m.y.; cf. Malinverno et al., 2010) and formed during the OAE 1a interval, although we cannot confidently exclude the possibility that the onset of deposition was as early as Barremian.

The current view is that the South Atlantic evaporites were deposited between 116 and 111 Ma in the late Aptian–earliest Albian interval (Davison, 2007; Chaboureaud et al., 2013; Gomes et al., 2016; time scale of Ogg et al., 2012), ~4–13 m.y. after OAE 1a (cf. Bottini et al., 2012). This interpretation is based on the stratigraphic relationships between the evaporites and supposedly extrusive rocks with Ar-Ar ages of 117 Ma (cited in Moreira et al., 2007) and 113.2 ± 0.1 Ma (cited in Dias et al., 1994). However, no details are available as to whether the dated samples are from pristine or altered rocks, and detailed analytical methodologies are not reported. In addition, this evidence alone is at odds with the presence of lower Aptian ammonites (*Dufrenoyia justinae*) described by Bengtson et al. (2007) from supraevaporite sediments in the Sergipe-Alagoas Basin (Fig. 1), and the record of lower Aptian planktonic foraminifera (presence of *Leopoldina cabri*) in supraevaporite sediments from the African side, offshore Angola (Davison, 2007). These associations suggest that evaporite deposition took place, at least locally, before or during the early Aptian. It is significant that the new stratigraphic correlation for the evaporites from the Campos and Santos Basins with OAE 1a corresponds closely with the well-dated ages of those from the African margin and Sergipe-Alagoas Basin, onshore northeastern Brazil, suggesting a similar age for these sediments across the entire central segment of the South Atlantic Ocean.

Important evidence for the age of the evaporites is offered by sulfur isotope values ( $\delta^{34}\text{S}$ ) between ~17‰ and ~22‰, obtained from anhydrite of the Santos Basin (blue rectangle in Fig. 2; Santos Neto et al., 2013), that can be compared to  $\delta^{34}\text{S}$  values from barite and carbonate-associated sulfate in sediments worldwide (red data in Fig. 2). The values from the Santos Basin evaporites are higher than the range of  $\delta^{34}\text{S}$  values postdating OAE 1a (14‰–17‰) and lower than the highest values recorded in the latest late Barremian (24‰–25‰; Fig. 2). Therefore, they likely constrain evaporite deposition to the interval latest late Barremian–early Aptian, including OAE 1a.

The decrease in  $\delta^{34}\text{S}$  values recorded worldwide (Fig. 2) coincides with the characteristic pattern in  $\delta^{13}\text{C}$  profiles during OAE 1a, i.e., a negative excursion followed by the onset of a positive excursion (e.g., Gomes et al., 2016).

Formation of the Ontong Java Plateau probably released massive amounts of CO<sub>2</sub> and SO<sub>2</sub> during basalt-seawater interaction, both relatively <sup>34</sup>S and <sup>13</sup>C depleted, which could explain low  $\delta^{34}\text{S}$  and  $\delta^{13}\text{C}$  values at the onset of OAE 1a (e.g., Paytan et al., 2004; Méhay et al., 2009). However, it cannot explain the decoupling between  $\delta^{34}\text{S}$  and  $\delta^{13}\text{C}$  profiles, whereby the positive excursion in  $\delta^{13}\text{C}$  occurs with relatively low  $\delta^{34}\text{S}$  values during and after OAE 1a. This pattern is in marked contrast with positive excursions in both  $\delta^{13}\text{C}$  and  $\delta^{34}\text{S}$  profiles of the Toarcian and Cenomanian–Turonian OAEs, when enhanced burial of organic matter and pyrite preferentially sequestered <sup>12</sup>C and <sup>32</sup>S, respectively (Gill et al., 2011; Gomes et al., 2016). Geochemical models indicate that burying a huge volume of gypsum and/or anhydrite in the South Atlantic would have led to a reduction of the global concentration of sulfate, limiting pyrite burial and enhancing organic-matter preservation, which could explain this behavior of  $\delta^{34}\text{S}$  and  $\delta^{13}\text{C}$  profiles during and after OAE 1a (Wortmann and Chernyavsky, 2007).

In summary, our new stratigraphic revision suggests that deposition of the South Atlantic evaporites, after the release of CO<sub>2</sub> and SO<sub>2</sub> during the formation of the Ontong Java Plateau, may have removed massive amounts of sulfate from the world ocean, decreasing global pyrite burial, increasing average marine organic-matter preservation worldwide, and leading to relatively elevated  $\delta^{13}\text{C}$  values and lower  $\delta^{34}\text{S}$  values in sediments deposited during and after the end of OAE 1a.

#### ACKNOWLEDGMENTS

We acknowledge Petrobras (Brazil) for support and permission to publish this research. We thank the reviewers for their helpful comments on the manuscript.

#### REFERENCES CITED

- Azevedo, R.L.M., 2001, O Albiano no Atlântico sul: Estratigrafia, paleoceanografia e relações globais [Ph.D. thesis]: Porto Alegre, Brazil, Universidade Federal do Rio Grande do Sul, 265 p.
- Azevedo, R.L.M., Gomide, J., Viviers, M.C., and Hashimoto, A.T., 1987, Biostratigrafia do Cretáceo marinho da Bacia de Campos: *Revista Brasileira de Geociências*, v. 17, p. 147–153.
- Bengtson, P., Koutsoukos, E.A.M., Kakabadze, M.V., and Zucon, M.H., 2007, Ammonite and foraminiferal biogeography and the opening of the Equatorial Atlantic gateway: 1st International Palaeobiogeography Symposium, Résumés, Abstracts, p. 12.
- Bottini, C., Cohen, A.S., Erba, E., Jenkyns, H.C., and Coe, A.L., 2012, Osmium-isotope evidence for volcanism, weathering, and ocean mixing during the early Aptian OAE 1a: *Geology*, v. 40, p. 583–586, doi:10.1130/G33140.1.
- Bottini, C., Erba, E., Tiraboschi, D., Jenkyns, H.C., Schouten, S., and Sinninghe Damsté, J.S., 2015, Climate variability and ocean fertility during the Aptian Stage: *Climate of the Past*, v. 11, p. 383–402, doi:10.5194/cp-11-383-2015.
- Bralower, T.J., CoBabe, E., Clement, B., Sliter, W.V., Osburn, C.L., and Longoria, J., 1999, The record of global change in Mid-Cretaceous (Barremian–Albian) sections from the Sierra Madre, northeastern Mexico: *Journal of Foraminiferal Research*, v. 29, p. 418–437.
- Chaboureaud, A.-C., Guillocheau, F., Robin, C., Rohais, S., Moulin, M., and Aslanian, D., 2013, Paleogeographic evolution of the central segment of the South Atlantic during Early Cretaceous times: Paleotopographic and geodynamic implications: *Tectonophysics*, v. 604, p. 191–223, doi:10.1016/j.tecto.2012.08.025.
- Davison, I., 2007, Geology and tectonics of the South Atlantic Brazilian salt basins, in Ries, A.C., et al., eds., *Deformation of the continental crust: The legacy of Mike Coward*: Geological Society of London Special Publication 272, p. 345–359, doi:10.1144/GSL.SP.2007.272.01.18.
- Davison, I., Anderson, L., and Nuttall, P., 2012, Salt deposition, loading and gravity drainage in the Campos and Santos salt basins, in Alsop, G.I., et al., eds., *Salt tectonics, sediments and prospectivity*: Geological Society of London Special Publication 363, p. 159–174, doi:10.1144/SP363.8.
- Dias, J.L., 1998, Análise sedimentológica e estratigrafia do Andar Aptiano em parte da margem leste do Brasil e no platô das Malvinas—Considerações sobre as primeiras incursões e ingressões marinhas do Oceano Atlântico Meridional [Ph.D. thesis]: Porto Alegre, Brazil, Universidade Federal do Rio Grande do Sul, 208 p.
- Dias, J.L., Sad, A.R.E., Fontana, R.L., and Feijó, F.J., 1994, Bacia de Pelotas: *Boletim de Geociências da Petrobras*, v. 8, p. 235–245.
- Gill, B.C., Lyons, T.W., and Jenkyns, H.C., 2011, A global perturbation to the sulfur cycle during the Toarcian Oceanic Anoxic Event: *Earth and Planetary Science Letters*, v. 312, p. 484–496, doi:10.1016/j.epsl.2011.10.030.
- Gomes, M.L., Hurtgen, M.T., and Sageman, B.B., 2016, Biogeochemical sulfur cycling during Cretaceous oceanic anoxic events: A comparison of OAE1a and OAE2: *Paleoceanography*, v. 31, p. 233–251, doi:10.1002/2015PA002869.
- Herrle, J.O., Schröder-Adams, C.J., Davis, W., Pugh, A.T., Galloway, J.M., and Fath, J., 2015, Mid-Cretaceous High Arctic stratigraphy, climate, and Oceanic Anoxic Events: *Geology*, v. 43, p. 403–406, doi:10.1130/G36439.1.
- Huber, B.T., and Leckie, R.M., 2011, Planktic foraminiferal species turnover across deep-sea Aptian/Albian boundary sections: *Journal of Foraminiferal Research*, v. 41, p. 53–95, doi:10.2113/gsjfr.41.1.53.
- Jenkyns, H.C., 2010, Geochemistry of oceanic anoxic events: *Geochemistry, Geophysics, Geosystems*, v. 11, Q03004, doi:10.1029/2009GC002788.
- Malinverno, A., Erba, E., and Herbert, T.D., 2010, Orbital tuning as an inverse problem: Chronology of the early Aptian oceanic anoxic event 1a (Selli Level) in the Cismon APITCORE: *Paleoceanography*, v. 25, PA2203, doi:10.1029/2009PA001769.
- Méhay, S., Keller, C.E., Bernasconi, S.M., Weissert, H., Erba, E., Bottini, C., and Hochuli, P.A., 2009, A volcanic CO<sub>2</sub> pulse triggered the Cretaceous Oceanic Anoxic Event 1a and a biocalcification crisis: *Geology*, v. 37, p. 819–822, doi:10.1130/G30100A.1.
- Menegatti, A.P., Weissert, H., Brown, R.S., Tyson, R.V., Farrimond, P., Strasser, A., and Caron, M., 1998, High-resolution  $\delta^{13}\text{C}$  stratigraphy through the early Aptian “Livello selli” of the Alpine Tethys: *Paleoceanography*, v. 13, p. 530–545, doi:10.1029/98PA01793.
- Moreira, J.L.P., Madeira, C.V., Gil, J.A., and Machado, M.A.P., 2007, Bacia de Santos: *Boletim de Geociências da Petrobras*, v. 15, p. 531–549.
- Norton, I.O., Carruthers, D.T., and Hudec, M.R., 2016, Rift to drift transition in the South Atlantic salt basins: A new flavor of oceanic crust: *Geology*, v. 44, p. 55–58, doi:10.1130/G37265.1.
- Ogg, J.G., Hinnov, L.A., and Huang, C., 2012, Cretaceous, in Gradstein, F.M., et al., eds., *The Geologic Time Scale 2012*: Boston, Elsevier, p. 793–853, doi:10.1016/B978-0-444-59425-9.00027-5.
- Paytan, A., Kastner, M., Campbell, D., and Thieme, M.H., 2004, Seawater sulfur isotope fluctuations in the Cretaceous: *Science*, v. 304, p. 1663–1665, doi:10.1126/science.1095258.
- Premoli Silva, I., and Verga, D., 2004, *Practical manual of Cretaceous planktonic foraminifera*: Perugia, Tipografia Pontefelcino, 283 p.
- Quintaes, C.M.S.P., 2006, Aplicação da estratigrafia química e da estratigrafia de seqüências na seção albiana da porção sul da Bacia de Santos [M.S. thesis]: Rio de Janeiro, Brazil, Universidade do Estado do Rio de Janeiro, 182 p.
- Sabato Ceraldi, T., and Green, D., 2017, Evolution of the South Atlantic lacustrine deposits in response to Early Cretaceous rifting, subsidence and lake hydrology, in Sabato Ceraldi, T., et al., eds., *Petroleum geoscience of the West Africa margin*: Geological Society of London Special Publication 438, p. 77–98, doi:10.1144/SP438.10.
- Santos Neto, E.V., Morais, E.T., Ferreira, A.A., and Torres, C.L., 2013, H<sub>2</sub>S risk in presalt reservoirs, OTC Brasil 2013: Rio de Janeiro, Brazil, Offshore Technology Conference, 4 p., doi:10.4043/24368-MS.
- Winter, W.R., Jahnert, R.J., and França, A.B., 2007, Bacia de Campos: *Boletim de Geociências da Petrobras*, v. 15, p. 511–529.
- Wissler, L., Funk, H., and Weissert, H., 2003, Response of Early Cretaceous carbonate platforms to changes in atmospheric carbon dioxide levels: *Palaeogeography, Palaeoclimatology, Palaeoecology*, v. 200, p. 187–205, doi:10.1016/S0031-0182(03)00450-4.
- Wortmann, U.G., and Chernyavsky, B.M., 2007, Effect of evaporite deposition on Early Cretaceous carbon and sulphur cycling: *Nature*, v. 446, p. 654–656, doi:10.1038/nature05693.

Manuscript received 12 December 2016  
 Revised manuscript received 10 February 2017  
 Manuscript accepted 13 February 2017

Printed in USA